



|                                  |  |
|----------------------------------|--|
| <b>Publication Year</b>          | 2016   |
| <b>Acceptance in OA</b>          | 2020-05-26T16:33:03Z   |
| <b>Title</b>                     | The Front-End of the NOEMA Interferometer  |
| <b>Authors</b>                   | Chenu, Jean-Yves, Navarrini, Alessandro, Bortolotti, Yves, Butin, Gilles, Fontana, Anne Laure, Mahieu, Sylvain, Maier, Doris, Mattiocco, Francois, Serres, Patrice, Berton, Marylene, Garnier, Olivier, Moutote, Quentin, Parioleau, Magali, Pissard, Bruno, Reverdy, Julien |
| <b>Publisher's version (DOI)</b> | 10.1109/TTHZ.2016.2525762  |
| <b>Handle</b>                    | <a href="http://hdl.handle.net/20.500.12386/25202">http://hdl.handle.net/20.500.12386/25202</a>  |
| <b>Journal</b>                   | IEEE TRANSACTIONS ON TERAHERTZ SCIENCE AND TECHNOLOGY  |
| <b>Volume</b>                    | 6  |

# The Front-End of the NOEMA Interferometer

J.Y. Chenu, A. Navarrini, Y. Bortolotti, G. Butin, A.L. Fontana, S. Mahieu, D. Maier, F. Mattiocco, *Member, IEEE*,  
P. Serres, M. Berton, O. Garnier, Q. Moutote, M. Parioleau, B. Pissard, and J. Reverdy

**Abstract**— The IRAM Plateau de Bure Interferometer (PdBI) is being upgraded to a new powerful millimeter-wave radio astronomy facility called the Northern Extended Millimeter Array (NOEMA) which will double the number of the 15-m diameter antennas from six to 12. All antennas will be equipped with a new generation of dual-polarization Front-End covering the 72-373 GHz frequency range with four independent receivers integrated into a single cryostat.

All receivers utilize Sideband Separating (2SB) Superconductor-Insulator-Superconductor (SIS) mixers, each of which delivers two  $\sim 7.7$  GHz wide Intermediate Frequency (IF) outputs per polarization channel, thus increasing the total IF bandwidth which can be processed with a single setting of the interferometer from 8 GHz ( $2 \times 4$  GHz delivered by the existing PdBI Front-End) to  $\sim 31$  GHz ( $4 \times \sim 7.7$  GHz delivered by the NOEMA Front-End).

The first of the new NOEMA antennas (Ant. 7) has recently been completed and the first NOEMA Front-End successfully developed and installed in it. For the coming years, our goal is to upgrade all the Front-Ends currently installed on the six existing PdBI antennas to the new NOEMA standard and to build six additional ones (plus one spare) for the new NOEMA antennas.

In this paper, we describe the design, fabrication and assembly of the Front-End we have developed for NOEMA Antenna 7. The instrument has state-of-the-art performance and sets a new standard in the post-ALMA generation technology.

**Index Terms**—Couplers, Cryogenics, Local oscillators, Low-noise amplifiers, Millimeter wave circuits, Mixers, Optics, Receivers, Superconductors, Wideband.

## INTRODUCTION

NOEMA, the successor to the IRAM Plateau de Bure observatory [1] will be, once finished, the most powerful millimeter radio telescope in the Northern Hemisphere and one of the most advanced facilities for radio astronomy. Located in the French Alps on the wide and isolated Plateau de Bure at an elevation of 2550 meters, the observatory currently consists of seven antennas, each 15 meters in diameter. Each antenna is equipped with state-of-the-art high-sensitivity receivers. Two tracks, extending on a North-South

All authors are with IRAM (Institute de RadioAstronomie Millimétrique), 38406 Saint Martin d'Hères, France. Contact person : Jean Yves Chenu (e-mail: chenu@iram.fr, phone : +33(0)476824913).

and East-West axis, enable the antennas to be moved up to a maximum separation of 760 meters.

The NOEMA array will double the number of antennas of its predecessor from six to 12. The first of the new NOEMA antennas, Ant. 7, was inaugurated at the end of September 2014 and its commissioning started in February 2015. During the next few years the construction of the array will continue and five more antennas will follow, approximately one per year until 2019. By the end of 2019, NOEMA will see a dramatic performance increase. The interferometer will provide sensitivities very close to ALMA (Atacama Large Millimeter/submillimeter Array) [2]-[3], unprecedented broadband spectral coverage ( $\sim 31$  GHz), and high quality imaging with a spatial resolution down to 0.1". NOEMA capabilities will be key to developing a better understanding of galaxy evolution from the high- $z$  to the local Universe, unlocking the dynamical, physical and chemical complexities of planet and star formation processes in the Milky Way, determining the chemical properties and evolution of molecular clouds from which future solar systems are born, and along the way help understanding the emergence of life on Earth.

The two other major elements of the upgrade for the observatory are:

- the extension of the East-West baseline from  $\sim 0.8$  to  $\sim 1.6$  km;
- the increase of the total IF bandwidth, which can be observed with one single LO (Local Oscillator) setting, from 8 GHz to  $\sim 31$  GHz.

The latter specification has required re-designing the dual-polarization quadri-band PdBI Front-Ends, which have been in continuous operation since their installation in 2006. Specifically, the backshort-tuned Single Side Band (SSB) SIS mixers delivering 4 GHz IF bandwidth per polarization channel, currently adopted for PdBI Bands 1, 2, and 3 [4]-[5]-[6], are replaced with new Sideband Separating (2SB) mixers providing two  $\sim 7.7$  GHz wide IF bands (LSB and USB) per polarization channel [7] increasing the total IF band delivered to the correlator from  $2 \times 4$  GHz (8 GHz) to  $4 \times \sim 7.7$  GHz ( $\sim 31$  GHz). Also, the four RF bands of the NOEMA Front-End are larger than those of the current PdBI receiver generation. In particular, the Band 1 lower frequency edge is extended down to 72 GHz, thus allowing to cover important molecular lines not yet accessible to the ALMA.

The NOEMA project is organized in two phases: Phase A includes the construction of four new antennas (the first of the new antennas being Ant. 7, recently commissioned) with new Front-Ends and a new correlator for all antennas; Phase B includes the construction of two additional antennas with Front-Ends and the extension of the baselines. In the end, the project requires fabrication, construction, test, and installation of 12 identical Front-Ends (plus one spare) on the future 12 antennas of the NOEMA array. Our goal for Phase A is to upgrade the 7 (6+1 spare) existing PdBI Front-Ends and build 4 new ones within the NOEMA specification. All instruments, the upgraded and new ones, will be built from identical parts and are expected to deliver similar performances.

The execution of the series production of 13 state-of-the-art multi-band NOEMA Front-Ends, with tight performance and schedule constraints for each sub-assembly, is benefitting from the organization which was put in place, within the IRAM Front-End group, during the production of the 73 ALMA Band 7 (275-373 GHz) receiver cartridges [8]

The article is organized as follows. In Sect. II we give the top level requirements for the NOEMA Front-End and a breakdown into subsystems and their functions by outlining the main novelties and improvements with respect to the existing PdBI Front-End. The details of the instrument subsystems are given in Sect. III. In Sect. IV we present the laboratory experimental results of the first Front-End we have built for NOEMA, while in Sect. V we illustrate its installation in Ant. 7. Finally, we conclude by describing the possible upgrades of the system in Sect. VI.

#### NOEMA FRONT-END: SYSTEM OVERVIEW

The main NOEMA Front-End requirements are the following:

- Four frequency bands with RF coverage shown in Table I, which also includes a comparison with the PdBI system.
- Sideband Separating (2SB) mixing scheme for all bands, with both the upper (USB) and lower (LSB) RF sidebands converted to separate IF outputs.
- IF bandwidth, per channel:  $\sim 7.7$  GHz.
- Dual polarization.
- One out of four RF frequency bands observable at the time (no dual-band/multi-band observations).
- Full remote control of all functions.
- No cryogenic fluid refills: closed-cycle cryocooler.

TABLE I  
BANDS DEFINITION AND SIS MIXER SCHEMES OF THE PdBI AND NOEMA FRONT-ENDS

| Band | Current PdBI Front-End |          |              | NOEMA Front-End |              |              |
|------|------------------------|----------|--------------|-----------------|--------------|--------------|
|      | RF [GHz]               | IF [GHz] | Mixer scheme | RF [GHz]        | IF [GHz]     | Mixer scheme |
| 1    | 83-116                 | 4-8      | SSB          | 72-116          | 3.872-11.616 | 2SB          |
| 2    | 129-174                | 4-8      | SSB          | 127-179         | 3.872-11.616 | 2SB          |
| 3    | 200-268                | 4-8      | SSB          | 200-276         | 3.872-11.616 | 2SB          |
| 4    | 277-371                | 4-8      | 2SB          | 275-373         | 3.872-11.616 | 2SB          |

More detailed specifications of the NOEMA Front-End, given in Table II, include those on the Single Side Band receiver noise

temperature, of order few-times the quantum limit, and on the image band suppression, 10 dB with allowance for all bands.

The NOEMA Front-End system design and architecture were described in [9]-[10]. A block diagram of the instrument, given in Fig. 1, shows: *a*) the optics, at room and cryogenic temperature, which includes cryogenic optics modules with polarization splitting wire grids, mirrors and feed-horns for the different bands; *b*) the dewar, which includes the SIS mixers and cryogenic IF sections with IF hybrid couplers, isolators and HEMT (High Electron Mobility Transistor) Low Noise Amplifiers (LNAs); *c*) the warm IF section (outside the dewar), which includes the IF switches and room temperature amplifiers; *d*) the local oscillator system, which includes the LO racks and external frequency multipliers.

A 3D view of the inner part of the NOEMA Front-End is shown in Fig. 2, while Fig. 3 illustrates the details of one of the four RF cryogenic optics modules (Band 1). The instrument architecture is based on the successful designs of the quadri-band PdBI and EMIR (Eight-Mixer Receiver [11]-[12]) Front-Ends, the latter being deployed on the IRAM 30-m radiotelescope [13]. The NOEMA instrument features many novelties and improvements over the two above mentioned Front-Ends, in particular over the PdBI one. The most important improvements are the following: an improved thermalization of the cryogenic stages allowing quicker warm-up/cooling down cycles, improved optics, new mixers, new wider band IF sections at cryogenic and room temperatures, new optical-fiber laser rack for the IF signals, new local oscillator systems, improved calibration loads, and new control electronics.

The electronically tuned local oscillator system employed to pump the NOEMA SIS mixers is described with details in separate articles, [14]-[15].

It was decided to keep the Band 4 receiver module currently used in the PdBI cryostat, which delivers 4 GHz IF band per polarization channel. This is based on an ALMA Band 7 2SB SIS mixer with one IF sideband internally terminated into a matched load. It is foreseen to upgrade the Band 4 receiver in the near future.

The production of 13 NOEMA Front-Ends (12 plus one spare) requires the design, fabrication, validation and procurement of a large amount of sub-assemblies. The main elements composing each Front-End are the following (details will be discussed in next section):

- $1 \times$  cryostat (plus its supporting frame), including a closed-cycle cryocooler and compressor;
- $4 \times$  dual-polarization cryogenic modules (one for each RF band), each of which comprises two refocusing mirrors, a wire-grid and two feed-horns;
- $8 \times$  2SB SIS mixer/IF hybrid coupler assemblies (two per band);
- $4 \times$  waveguide LO polarization splitters (one for each RF band);
- $16 \times$  cryogenic isolators and  $16 \times$  Low Noise Amplifiers (LNAs) for the  $\sim 3.8$ - $11.7$  GHz IF band;
- $6 \times$  vacuum windows and as many Infrared (IR) filters for the different RF bands (one for each signal path of the four RF bands, one for each calibration path of the two calibration loads);

- 4 × warm IF amplification modules for the ~3.8-11.7 GHz IF band. Each module includes a four-way switch, two room-temperature LNAs, a variable digital attenuator with integrated equalizer, a filter, a detector and other microwave components;
- 1 × laser rack with four laser emitters and two switches for the transportation of the IF signal and the switching of the polarization (for polarimetry use). The laser rack includes a new EtherCat board for monitoring and control;
- 3 × local oscillator racks (and their power supply): two independent racks to pump the Band 1 and the Band 4 SIS mixers, and one rack to

pump either the Band 2 or the Band 3 SIS mixers through a waveguide switch;

- Commercial frequency multipliers<sup>1</sup> to generate the final LO frequency signal injected at the waveguide ports of the cryostat: a doubler for Band 2, and two triplers (one for Band 3 and one for Band 4).
- Waveguide filters for the rejection of the unwanted spurious harmonics of the LO.

Additional elements which are part of each Front-End are: the inner shields of the dewar, the flexible thermal links at each stage to reduce the mechanical vibrations, the high thermal conductivity OFHC (Oxygen-Free High Conductivity) copper links for the thermalization of the components at 4 K, the coaxial cables (in copper and stainless steel) for the IF signals transportation, the vacuum feedthroughs, the waveguide pieces (single-mode and over-moded) for the interconnection of the components, the cryogenic temperature sensors, the two motorized carousels with mirrors that select the calibration loads, the brass wires for dc biasing the SIS mixers and LNAs, the harnesses and connectors.

TABLE II  
NOEMA FRONT-END MAIN PERFORMANCE REQUIREMENTS

| Parameter   | Band 1  | Band 2  | Band 3  | Band 4  |
|---|---|---|---|---|
| <b>RF port freq. range</b>  | 72-116 GHz  | 127-179 GHz   | 200-276 GHz   | 275-373 GHz   |
| <b>LO port freq. range</b>  | 82-108.3 GHz  | 138.6-171.3 GHz   | 207.7-264.4 GHz   | 283-365 GHz   |
| <b>IF band</b>  | 3.8-11.7 GHz 2SB  | 3.8-11.7 GHz 2SB  | 3.8-11.7 GHz 2SB  | 3.8-11.7 GHz 2SB  |
| <b>Polarization states</b>  | Orthogonal linear   | Orthogonal linear   | Orthogonal linear   | Orthogonal linear   |
| <b>SSB receiver noise measured at the dewar window</b>            | <50 K 80% of RF band<br><70 K full RF band  | <65 K 80% of RF band<br><108 K full RF band   | <83 K 80% of RF band<br><138 K full RF band   | <147 K 80% of RF band<br><221 K full RF band  |
| <b>Image band suppression</b>                                     | >10 dB with allowance:<br>No more than 10%<10 dB<br>No more than 1%<7 dB<br>globally over all LO settings | >10 dB with allowance:<br>No more than 10%<10 dB<br>No more than 1%<7 dB<br>globally over all LO settings | >10 dB with allowance:<br>No more than 10%<10 dB<br>No more than 1%<7 dB<br>globally over all LO settings | >10 dB with allowance:<br>No more than 10%<10 dB<br>No more than 1%<7 dB<br>globally over all LO settings |
| <b>Integrated IF output power at fiber-optic link transmitter</b> | <-30 dBm  | <-30 dBm  | <-30 dBm  | <-30 dBm  |
| <b>Total IF power over 10 MHz-18 GHz</b>                          | No more than 3 dB higher than max in-band IF power  | No more than 3 dB higher than max in-band IF power  | No more than 3 dB higher than max in-band IF power  | No more than 3 dB higher than max in-band IF power  |
| <b>IF power variations, when measured with 10 MHz res.</b>        | 8 dB peak-to-peak full band   | 8 dB peak-to-peak full band   | 8 dB peak-to-peak full band   | 8 dB peak-to-peak full band   |
| <b>Output IF channel VSWR</b>                                     | 1.4:1   | 1.4:1   | 1.4:1   | 1.4:1   |
| <b>Large signal gain compression @ 300 K input</b>                | <5%   | <5%   | <5%   | <5%   |
| <b>Amplitude stability: Allan variance 0.05 s ...100...300 s</b>  | $4.0 \times 10^{-7}$ , $3.0 \times 10^{-6}$ , respectively  | $4.0 \times 10^{-7}$ , $3.0 \times 10^{-6}$ , respectively  | $4.0 \times 10^{-7}$ , $3.0 \times 10^{-6}$ , respectively  | $4.0 \times 10^{-7}$ , $3.0 \times 10^{-6}$ , respectively  |
| <b>Signal path phase stability over 300 sec</b>                   | <1 degree   | <1 degree   | <1 degree   | <1 degree   |
| <b>Aperture efficiency</b>  | >80%  | >80%  | >80%  | >80%  |
| <b>Focus efficiency</b>   | >98%  | >98%  | >98%  | >98%  |
| <b>Taper at the sub-reflector edge</b>                            | -11/-14 dB  | -11/-14 dB  | -11/-14 dB  | -11/-14 dB  |
| <b>Cross polarization</b>   | <-23 dB   | <-23 dB   | <-23 dB   | <-23 dB   |
| <b>Beam squint</b>  | <1/10 FWHM  | <1/10 FWHM  | <1/10 FWHM  | <1/10 FWHM  |

<sup>1</sup> From VDI (Virginia Diodes Inc.), Charlottesville, VA, USA.

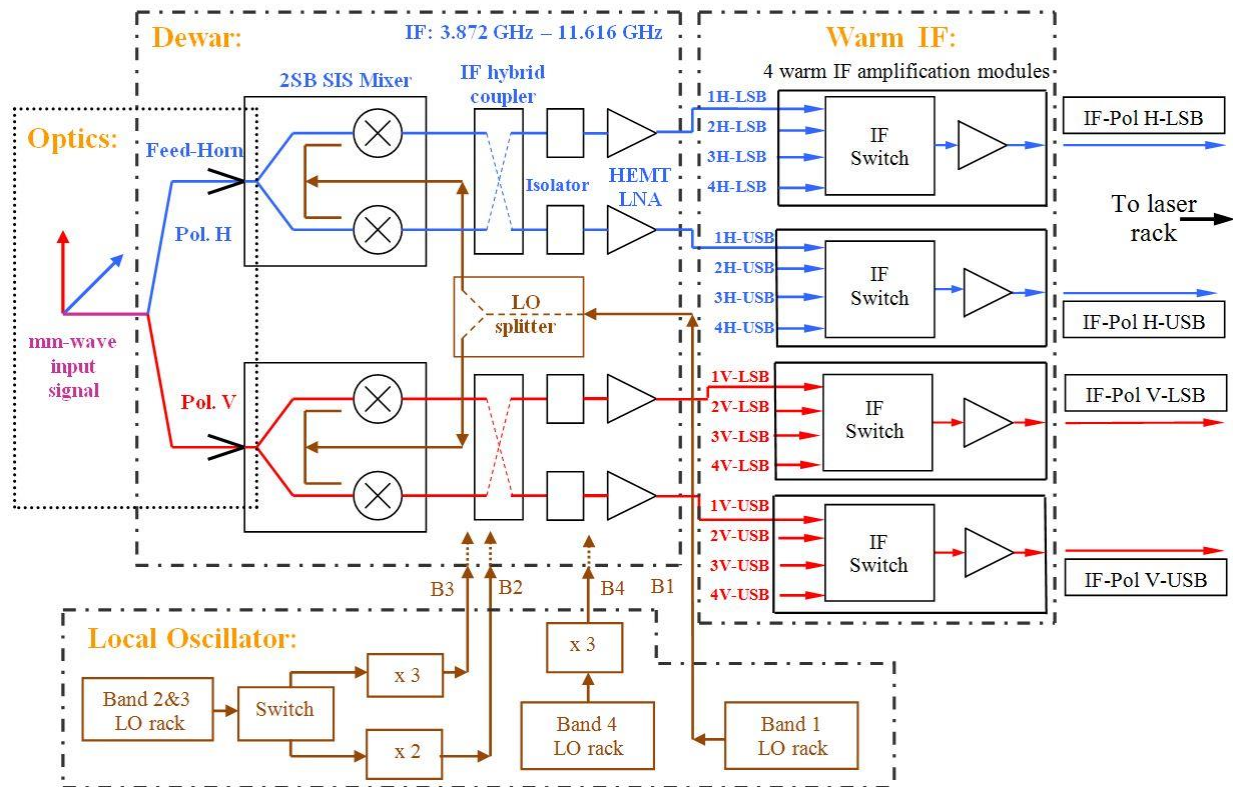


Fig. 1. Block diagram of the NOEMA Front-End showing the dual-polarization beam (Pol H in blue colour, Pol V in red colour) and the signal path through the main elements of one of the four selectable receiver bands. The signal propagates through the optics (including refocusing mirrors, polarization splitting wire grids and corrugated feed-horns) and through the mixers and cryogenic IF section inside the dewar. Out of the 16 available outputs, the four IFs from each RF band are selected at the dewar output by four independent switches located inside four warm IF amplification modules. The local oscillator system that drives the SIS mixers include LO modules and frequency multipliers. The calibration system and the laser rack cascaded with the warm IF chains are not represented.

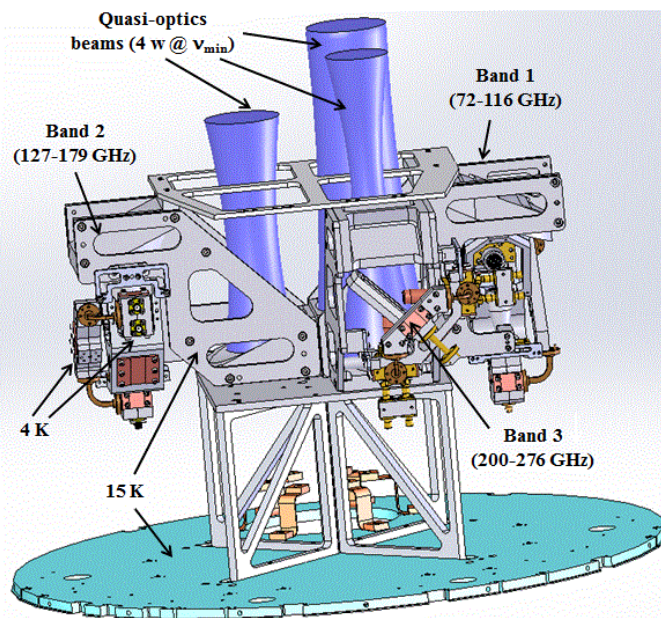


Fig. 2. 3D view of the inner part of the NOEMA Front-End showing three out of the four cryogenic RF optics modules (Band 1, 2 and 3) with their vertically oriented quasi-optics beams (represented with size of 4 times the beam waist at the minimum operating frequency in the respective band,  $v_{min}$ ).

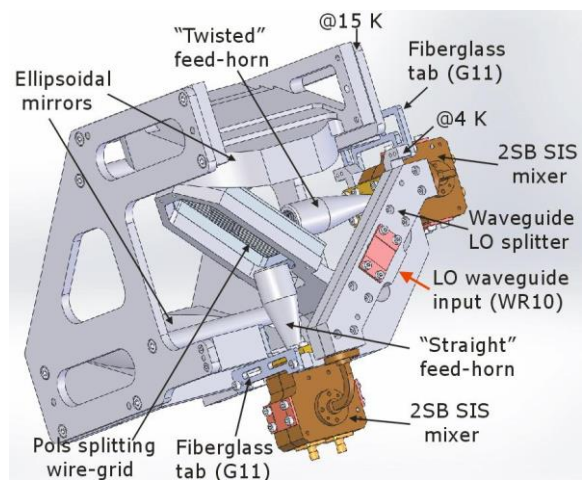


Fig. 3. 3D view of the NOEMA Band 1 (72-116 GHz) cryogenic optics module, assembled with two 2SB SIS mixers and a waveguide LO splitter (all thermalized at 4 K).

To give an estimate of the production line required by the project we emphasize that a total of  $\sim 100 \times$  2SB SIS mixer assemblies and of  $\sim 50 \times$  cryogenic optics modules, designed, fabricated, assembled and tested at IRAM, are required to complete all NOEMA Front-Ends. In addition, we note that, besides the cryostats, the cryo-coolers,  $\sim 200 \times$  cryogenic isolators,  $\sim 200 \times$  cryogenic LNAs, and  $\sim 100 \times$  room-temperature LNAs have to be procured.

## NOEMA FRONT-END SUBSYSTEMS

Details of some of the NOEMA Front-End subsystems are presented in the following subsections.

### A. Dewar

The cryogenic system adopted for the NOEMA Front-End is the same as the one currently adopted at PdBI, which is based on a closed-cycle cryocooler (Sumitomo model SRDK3ST) with three cryogenic stages at 80 K, 15 K and 4 K. The NOEMA cryostat vacuum enclosure and inner IR screens at 80 K and 15 K have the same size as those of the PdBI Front-End. The vacuum enclosure, made of aluminium, has a cylindrical shape with external diameter of 670 mm and height of ~550 mm.

### B. Optics

The interfaces of the optics subsystem are: at the input, the  $f/D \sim 5.1$  Cassegrain focus of the 15 m telescope (hyperbolic secondary mirror with diameter of 1.55 m and magnification 15.7); at the output, the waveguide flange between each corrugated horn and the corresponding mixer input. There are eight outputs (four frequency bands, dual polarization), one for each mixer. Between these interfaces, the optics subsystem realizes the following functions:

- match the telescope exit pupil (located at the subreflector) to the mouth of the corrugated horn through refocusing mirrors, and match the horn to its output rectangular waveguide, where a single fundamental  $TE_{10}$  mode propagates across the specified band;
- steer each of the two linear polarizations to an individual mixer thermalized to the ~4 K stage of the cryostat;
- let pass the RF signals through four independent vacuum windows and IR filters, which block the radiation that would otherwise add thermal load to the inner stages;
- perform a calibration of system gain and noise by the two-load method.

If we exclude the calibration elements, the optics subsystem comprises the vacuum windows, the IR filters and the cryogenic optics modules described below.

1) *Vacuum windows and IR filters:* The RF signals of the four bands enter the NOEMA Front-End through four independent HDPE vacuum windows and PTFE Infrared filters of improved design (Fig. 4) with respect to the ones used in the PdBI Front-End. A broadband matching layer with low reflection coefficient is achieved for all bands with triangular grooves machined into each dielectric surface with angle  $\alpha = 20^\circ$  and appropriate pitch (P) and height (H) that avoid the appearance of spurious modes (see Table III). Corrugations on one face are perpendicular to those on the other face to avoid artificial birefringence. All vacuum windows and IR filters have a disk-like shape with size and central thickness calculated for each RF band to avoid beam truncation at a level of less than 0.5% and hold the vacuum pressure (for vacuum windows).



Fig. 4. Photo of HDPE vacuum window showing the triangular grooves on one of the surfaces (left). Geometry of the corrugations (right).

TABLE III  
PITCH (P) AND HEIGHT (H) OF TRIANGULAR GROOVES

|        | Band 1 | Band 2 | Band 3 | Band 4 |
|--------|--------|--------|--------|--------|
| P [mm] | 1.693  | 1.058  | 0.705  | 0.529  |
| H [mm] | 4.8    | 3      | 2      | 1.5    |

2) *Cryogenic optics modules:* improved cryogenic optics modules were designed (shown in Figs. 2-3), fabricated and tested for Bands 1, 2 and 3 in order to cover the large NOEMA RF bandwidths. All modules share the same design philosophy, similar to that adopted in the existing PdBI receivers, where two ellipsoidal mirrors thermalized at 15 K re-image the antenna sub-reflector into the apertures of the two independent single-polarization feed-horns. A photo of one of the NOEMA Band 3 cryogenic optics module we fabricated and assembled is shown in Fig. 5. The modules are more lightweight and compact than the previous ones. A polarization splitting wire-grid and the two feed-horns, attached to the main frame of the module, are maintained at 4 K. Fiberglass tabs are used to thermally split the 15 K and the 4 K stages. The cryogenic optics modules for the other NOEMA bands use a similar architecture as shown in Fig. 6, top panel.

For each band, two types of feed-horns are used to ease the mechanical assembly with other cryogenic components, one with straight and the other with twisted waveguide output, as illustrated in the insets on top of Fig. 7. The result of the 3D electromagnetic simulation of the two types of NOEMA Band 1 corrugated feed-horns, performed with a commercial

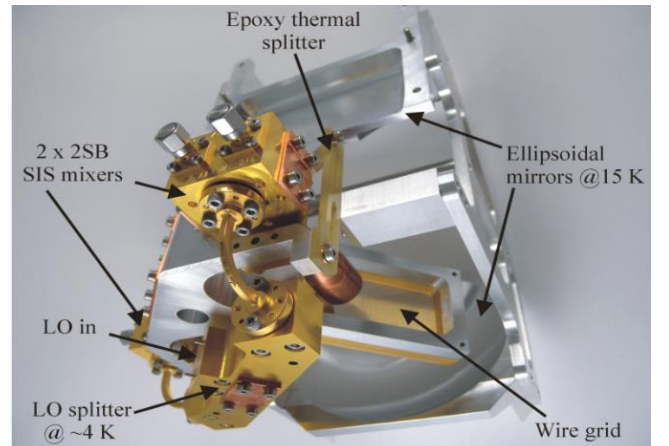


Fig. 5. NOEMA Band 3 cryogenic optics module assembled with LO waveguide splitter and two 2SB SIS mixers.

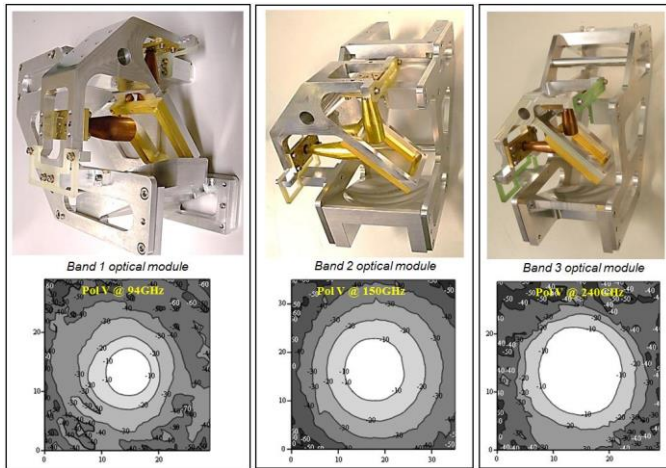


Fig. 6. Cryogenic optics modules for NOEMA Bands 1, 2 and 3 (top panels) and Pol V copolar beam patterns measured with the antenna range near the central frequency of the respective RF ranges (bottom panels).

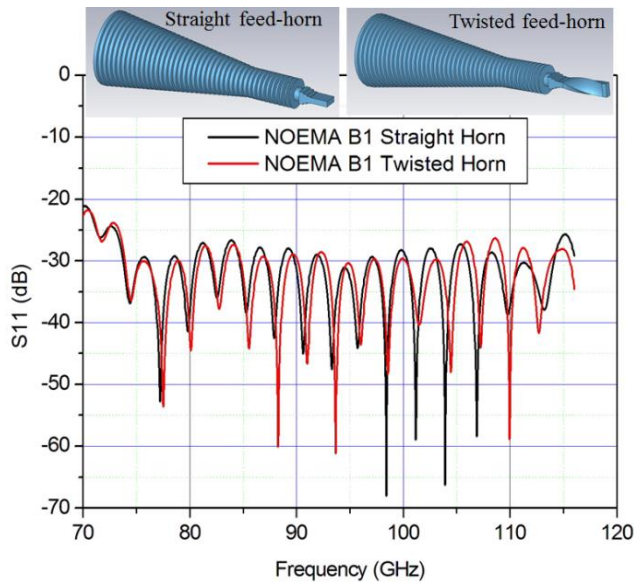


Fig. 7. Simulated input reflection coefficients of the corrugated “straight” and “twisted” feed-horns for NOEMA Band 1. The experimental results match closely the simulation values. The two insets show views of the “straight” and “twisted” feed-horns.



Fig. 8. Photo of some of the NOEMA Band 2 corrugated feed-horns.

software<sup>2</sup>, is shown on Fig. 7. The feeds were optimized across the 72-116 GHz band and fabricated by copper electroforming of a single aluminium mandrel which was subsequently etched away. Following the machining of the copper to its final external shape and size, a UG387 waveguide flange with rectangular shape, adapted for bolting with the cryogenic module, was inserted, aligned and glued at the feed-horn output. The Band 1 feeds have a simulated reflection below -25 dB which matches closely the measurements obtained with the IRAM Millimeter Vector Network Analyzer (MVNA).

Some of the feed-horns fabricated for NOEMA Band 2 are shown in Fig. 8.

The optics modules were tested at room temperature using the IRAM mm-wave antenna range as well as at their operating temperature inside the fully assembled receiver. They proved to work well, according to the prescribed specifications. The co- and cross-polarization beam-patterns of each polarization channel were measured near the central RF frequency and at the band edges. Co-polar beam-patterns of the modules measured at room temperature are shown in Fig. 6, bottom panel. The sidelobe and the cross-polarization levels are less than -20 dB for all bands.

The beams of the four RF bands point to different directions in the sky, thus only one band can be observed at any one time by pointing at an astronomical source.

### C. Sideband Separating SIS Mixers

The astronomical signals at the output of the horns are injected into the SIS mixers along with the strong monochromatic signals coming from the local oscillator system (to be described later on). The mixers perform the following operations: *a*) down-convert a frequency slice of one of the four RF bands (mm-wave) to the IF band (microwave band, ~3.8–11.7 GHz), with a minimum of added noise; *b*) separate the two side bands (LSB and USB), meaning that each of the two IF outputs contains the mixing product from only one of the RF side bands, with minimum contamination from the image band (rejection ratio >10 dB).

A key component of each mixer is one or several superconductor tunnel (SIS) junctions, consisting of a very thin layer of Al-AIO<sub>x</sub> insulator (thickness of few nm) sandwiched between two Niobium (Nb) superconducting layers. The SIS junction(s) of the NOEMA mixers are fabricated at the IRAM SIS Group laboratories. The junctions sit on top of a chip supported by fused quartz (see [8]) with a thickness of the order of ~100 μm. The SIS mixer chips are integrated in the mixer blocks, embedded in a waveguide channel. Fully integrated sideband separating SIS mixers have been developed for NOEMA Band 1 and 2. These mixers employ a completely planar IF coupler chip based on

<sup>2</sup> CST Microwave Studio: Computer Simulation Technology, Bad Nauheimer Str. 19 64289 Darmstadt Germany.

Niobium (Nb) striplines, which made it possible to integrate all components of the 2SB mixer, i.e. RF coupler, LO splitter, LO couplers, DSB mixers and IF coupler, into one E-plane split-block as shown in Figs. 9-10. The NOEMA Band 3 receivers are being equipped with a 2SB mixer previously developed within the European project AMSTAR+ [12]. All mixers have very broadband RF and IF performance achieving ultra-low noise and a flat response across the ~8 GHz wide IF band. A detailed description of the NOEMA mixers can be found in [5]. The SIS receivers performance are within the initial NOEMA specification, as will be shown in Sect. IV.

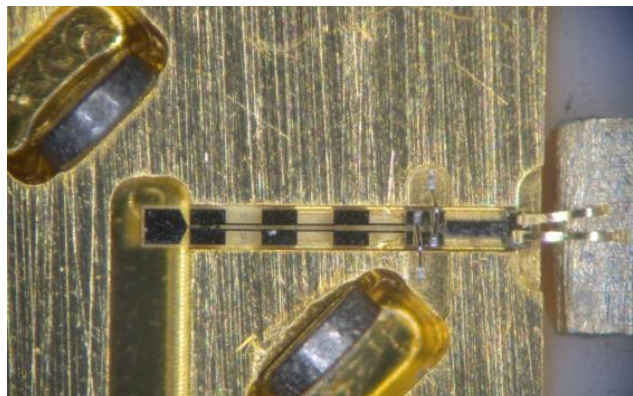


Fig. 9. Sideband Separating Mixer developed for NOEMA Band 3 (200-276 GHz) showing details of one of the two DSB mixer chips of the 2SB assembly with miniature magnets to suppress the Josephson effect.

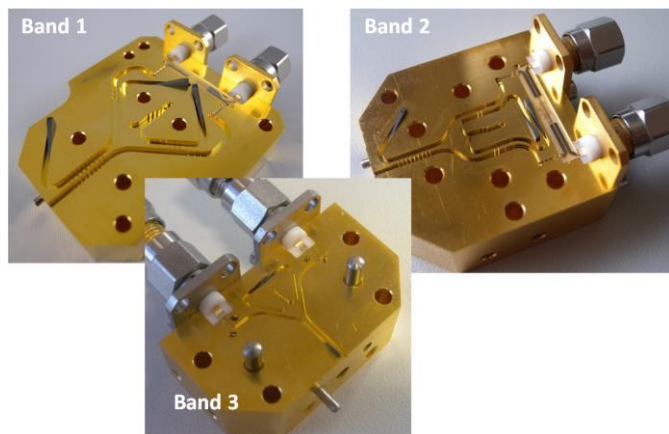


Fig. 10. Sideband separating SIS mixers for NOEMA Band 1, 2 and 3.

#### D. Local Oscillator system and injection scheme

The NOEMA LO system is described in [14]-[15]. It is based on commercial Yttrium Iron Garnet (YIG) oscillators operating in the ~15 GHz frequency range. The tuneable YIG signals drive the Active Multiplier Chains (AMCs), designed and produced at IRAM, which amplify, filter and multiply by 6 the input signal, thus delivering an LO in a suitable frequency (~90 GHz) and power range (>10 dBm). A photo of one of the AMCs developed for Band 1 is shown in Fig. 11.

For Band 1, the signal from the AMC output (in the range 82-110 GHz), pumps directly the 2SB SIS mixers (after being suitably attenuated and distributed).

For Band 4, the AMCs are cascaded with Power Amplifier (PA) modules, 3 dB power combiner modules, and commercial frequency triplers in order to generate the final LO frequency and required power level.

The AMCs and PAs employ commercially available MMICs and GaAs millimeter MMICs from NRAO (National Radio Astronomy Observatory) and are similar to those designed for ALMA [16]-[17]. All modules, except for the final frequency tripler, are assembled in a single rack as shown in Fig. 12 for the NOEMA Band 4 LO (eight units have been produced). Four of the production series NOEMA Band 1 LO racks are shown in Fig. 13 together with their power supply racks.



Fig. 11. Active Multiplier Chain developed for the NOEMA LO Band 1 system (AMC1) delivering a tuneable signal across ~82-108.3 GHz and a power level of order ~12 dBm at its WR10 waveguide output.

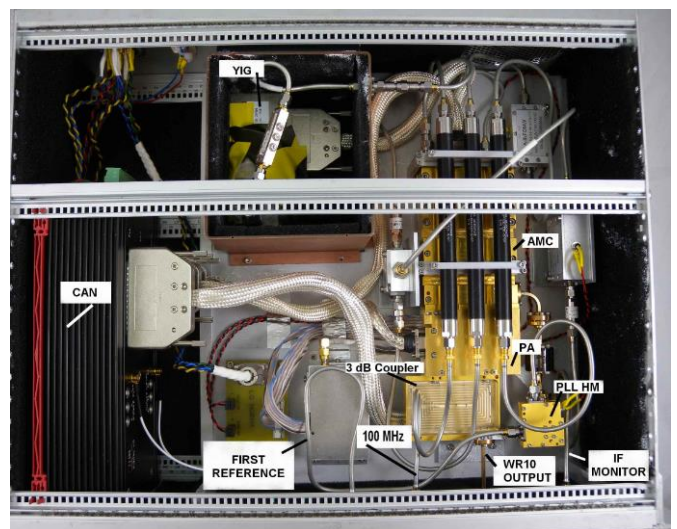


Fig. 12. The NOEMA Band 4 LO rack showing the CAN remote control interfaces, the YIG oscillator, the AMC, PA and 3 dB combination coupler, the PLL HM, the output WR8 waveguide flange.

The LO racks for Band 2&3 are based on a Gunn oscillator, rather than an electronically tuned active multiplier chain. The output of the common Band 2&3 module is

connected to a mechanical waveguide switch that diverts the LO tone from the rack, adjustable across the ~67-90 GHz band, to either a frequency doubler (for Band 2) or a frequency tripler (for Band 3).

Two Phase Locked Loop (PLL) reference signals (REF1, 13-16.4 GHz) from two independent modules employing four output connectors are available in the system. One module provides the first reference for Band 1, while the second module provides the reference for Band 2&3 and for Band 4.

Long waveguides (length of order 80 cm) are used to connect the three LO racks of each NOEMA Front-End (one for Band 1, one for Band 4, and a common one for Band 2&3), located on a support frame, to the frequency multipliers (used for Band 2, 3 and 4) located at cryostat input.

The multiplied chain of the LO system use active and passive multipliers which, in addition to the main (wanted) LO tone, might be source of unwanted harmonics at the SIS mixer LO input. Fig. 14 shows one of the ~134-184 GHz band pass filters we designed, fabricated and characterized to mitigate the LO spurious harmonics problem in Band 2. The filter is cascaded with the commercial frequency doubler



Fig. 13. The four production series of NOEMA Band 1 (~82-108.2 GHz) LO racks (right) and their power supply racks (left).

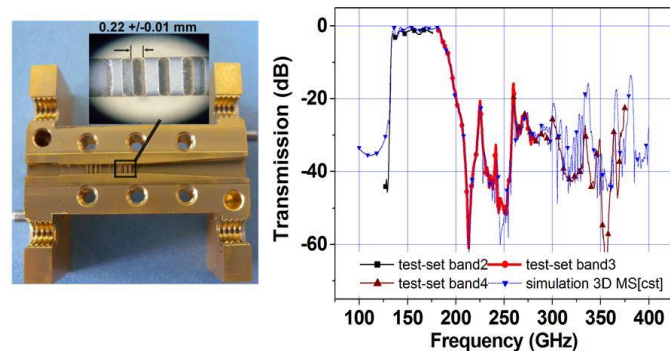


Fig. 14. LO Band 2 134-184 GHz band pass filter for spurious harmonics mitigation showing the detail of the waveguide structure (left). Filter response measured and modelled over the 100-375 GHz band (right).

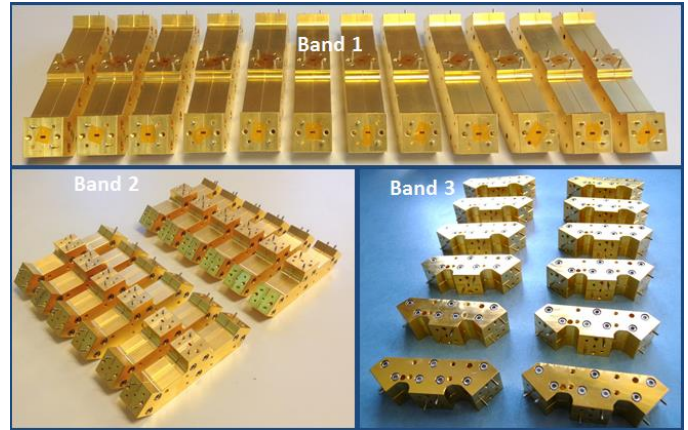


Fig. 15. Cryogenic LO splitters produced and characterized for NOEMA Bands 1, 2 and 3.

(with WR6 waveguide output, from VSI) and connected to the cryostat overmoded waveguide LO input port. Inside the cryostat, the LO signal propagates down to a waveguide splitter (shown in Fig. 5 and in Fig. 15) that divides equally the LO power and distributes it to the two orthogonal polarization channels.

#### E. IF section

The IF outputs of the 2SB mixers are connected to cryogenic isolators (operating at 4 K) and cascaded with cryogenic LNAs (operating at 15 K), which amplify the IF signal up to a level significantly above the noise of room temperature electronics. The NOEMA IF, 3.872-11.616 GHz, is a non-standard band and required a specific development of cryogenic LNAs and isolators (16 of each required to equip four bands of one Front-End). The development and production of the LNAs was subcontracted to CAY&TTI and that of the isolators to Quinstar/Pamtech.

The coaxial cables carrying the IF signals from the mixer/isolator/LNA cascade are arranged so that four groups of four IF feedthrough coaxial connectors are available at the cryostat output backplate, each group containing the signals from all bands (1, 2, 3 and 4), the different groups being Pol H-LSB, Pol H-USB, Pol V-LSB, Pol V-USB, as shown in the schematic of Fig. 1.

A room temperature IF amplification module (Fig. 16), connected on the backplate of the NOEMA cryostat, selects one of the four possible IFs from each of the four RF bands. Four of such modules are used in one Front-End. Each module includes an input switch which is cascaded with two low noise amplifiers, a band pass filter, and a digital attenuator with integrated equalizer that deliver a final IF signal in a suitable power range to the laser rack.

#### F. Laser rack

A new laser rack was developed to convert the  $4 \times \sim 3.8-11.6$  GHz IF signals from the four warm IF modules of



Fig. 16. Warm IF amplification module with integrated switch and digital attenuator.

each Front-End to optical (1330 nm wavelength) for their transportation to the correlator through optical fibers. The analog fiber optic links are made by Miteq. Two transfer switches (named polar switches) located inside the laser rack allow changing the polarization states by reversing the signals of Pol H and Pol V. The optimum input power at the laser emitter is of the order of  $-30$  dBm. A view of the laser rack is shown in Fig. 17.



Fig. 17. NOEMA laser emitter rack.

#### G. EtherCAT receiver control electronics

New bias modules for the LNAs and the SIS mixers, controlled by EtherCAT, are under development. They will replace the old control electronics based on I2C (Inter-Integrated Circuit) and CAN (Controller Area Network). One Front-End will use two EtherCat bias modules to control the 16 LNAs and one single EtherCAT SIS junction bias module for the  $8 \times 2$ SB mixers ( $16 \times$  SIS mixer chips). The warm IF and the laser rack as well as a new cryogenic temperature monitoring system are also controlled by the EtherCAT. Fig. 18 shows two of the modules under development. At the moment, the NOEMA Front-End for Ant. 7 employs the existing PdBI receiver control electronics which has been adapted to the new system.



Fig. 18. EtherCat modules for biasing the NOEMA SIS junctions (left) and controlling the warm IF chain and laser rack emitter (right).

#### H. Calibration

For each of the four RF bands, the dual-polarization receiver beams can be coupled to either an ambient temperature load or a cold load thermalized inside the cryostat at 15 K. The cold load is coupled through wideband low-loss HDPE window and IR PTFE filter by pairs of mirrors located in a carousel. Two carousels are employed, one for the Band 1&2 beams, the other for the Band 3&4 beams. The two ambient temperature loads are also located on the two carousels.

A wideband cryogenic calibration load based on pyramidal shaped sections on Eccosorb MF-114 material from Emerson&Cuming was successfully developed. The load has improved performance with respect to that of previous generation.

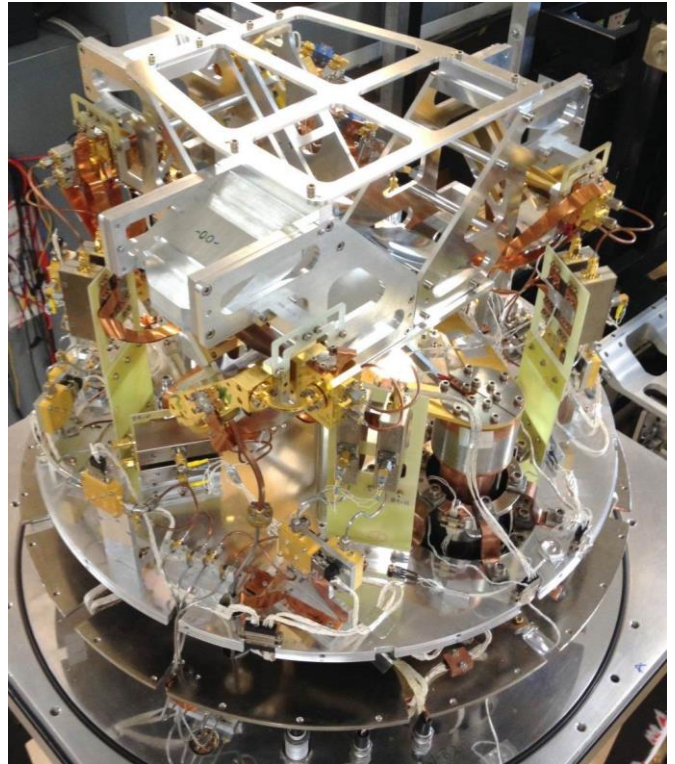


Fig. 19. View of the cold sections of the NOEMA Front-End.

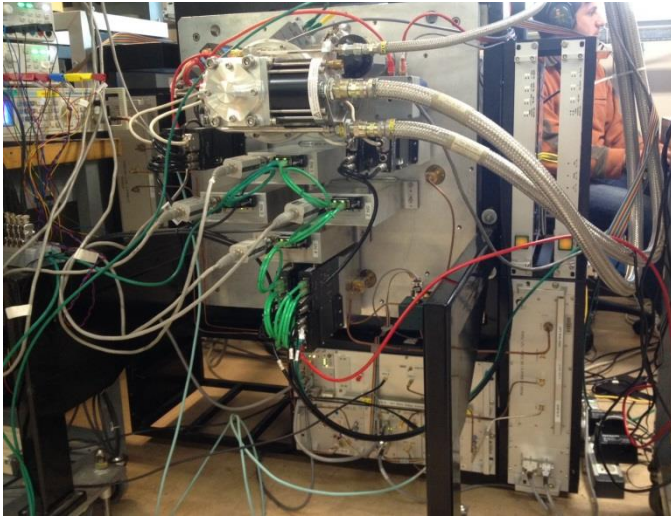


Fig. 20. View of the NOEMA Front-End showing the Sumitomo cold head, the four warm IF amplification chains attached to the cryostat backplate, the bias and control electronics modules for the SIS mixers and LNAs as well as the LO racks arranged together with other modules.

## I. EXPERIMENTAL RESULTS

First, the 2SB SIS mixers were assembled and individually characterized utilizing laboratory test cryostats (from Infrared Laboratories Inc.) with liquid nitrogen and liquid helium. Three of such cryostats are available, one per band, to speed up the mixers production. Beside the noise temperature, the laboratory receiver setup allowed us to measure the image band rejection with a Martin-Pupplett Interferometer, which filters out the image sideband.

Second, the mixers within specifications with similar performance and LO power requirements were selected and paired in dual-polarization cryogenic modules.

Third, the cryogenic optical modules (previously tested at room temperature) were assembled inside the cryostat and the construction of the Front-End was finalised. A photo of the inner cryogenic parts of the fully assembled NOEMA Front-End with the four RF bands is shown in Fig. 19.

Forth, the instrument was characterised in the laboratory, as shown in Fig. 20. The test results, presented below, shows that the instrument performance are within specification..

The noise performance were measured for each receiver band at a number of preliminarily specified LO frequency points. The 2SB receivers were optimized for each LO frequency by tuning the mixer bias voltage and the LO pumping power. After calibration of the internal cold load and setting of the variable attenuator of the warm IF module, the receiver noise was measured at each of the above indicated LO frequencies using the Y-factor method. All measurement results discussed in the following subsections refer to the prototype NOEMA Front-End, which was installed in Ant. 7 in December 2014. Detailed measurement results are presented for NOEMA Band 1, while for Bands 2, 3 and 4, only the main results are shown.

### A. NOEMA Band 1 characterization results

For each LO setting, the receiver noise was tuned for optimum performance by varying the LO power level and the bias voltage applied to the two DSB SIS mixers of each 2SB unit (the same voltage is applied to the two DSB mixers).

Fig. 21 shows the measured pumped IV curves (blue dashed and solid lines), IF output powers and resulting DSB receiver noise of one 2SB assembly (purple dotted line) versus mixer bias voltage. The integrated IF output powers (dotted red lines) are the responses of the receiver to room temperature and cryogenic loads. The LO frequency was 105 GHz. The optimum parameter, which gives stable operation with receiver noise of the order of 30 K, is obtained by biasing the series array of the three SIS junctions at 7.8 mV with a pumped current close to 20  $\mu$ A.

Fig. 22 shows the SSB noise temperature integrated across the IF band versus RF signal frequency of the NOEMA Band 1 (72-116 GHz) Pol. V receiver channel. The receiver noise was measured for 15 different LO frequencies across the 80-108 GHz LO range. Optimum performance was obtained with bias voltages applied in the 7.8-7.9 mV range (each DSB mixer chip utilizes a series array of three SIS junctions) and with pumping currents in the 14-20  $\mu$ A range (see Fig. 26 further down). Such values are valid for that particular mixer (Pol. V). The SSB receiver noise of Fig. 22 was derived by increasing the measured DSB noise value of 10% in order to account for the contribution of the finite mixer rejection (of order 10 dB, see below). The integrated SSB noise is within the 50 K specification across the full frequency band.

The Band 1 Pol.H receiver channel has a similar performance.

The SSB receiver noise across the IF band for the Pol V NOEMA Band 1 receiver is shown in Fig. 23. The noise is flat in the lower part of the IF band and increases

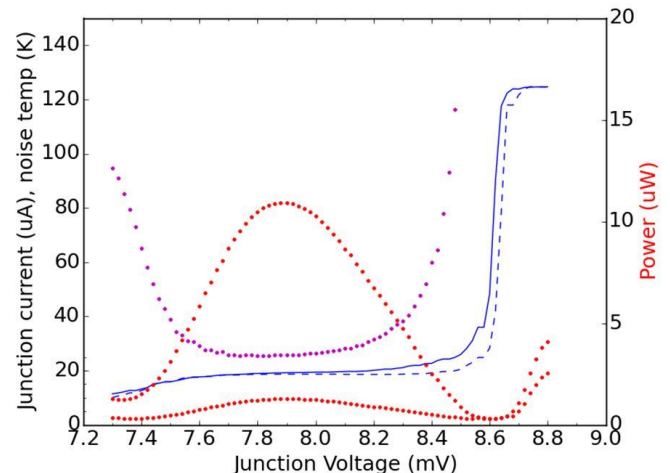


Fig. 21. Pumped IV curves (in blue), IF output powers in response to room temperature and cryogenic loads (in red) and receiver noise for LSB channel integrated across the IF band (purple) versus bias voltage applied to the series array of three SIS junctions. The LO frequency was 105 GHz.

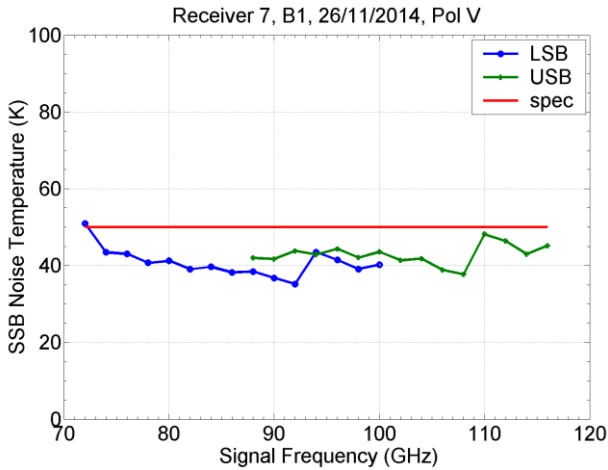


Fig. 22. SSB receiver noise temperature of the NOEMA Band 1 receiver, Pol. V, integrated across the IF band: LSB channel (blue line), USB channel (green line). The horizontal red line indicates the noise specification over 80% of the RF band.

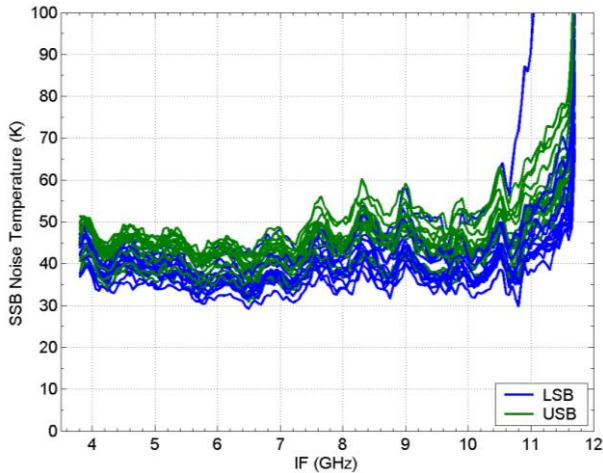


Fig. 23. Measured SSB receiver noise across the IF band for 15 LO tunings, one every 2 GHz, from 80 GHz to 108 GHz: LSB channel (blue line), USB channel (green line).

slightly towards the higher band edge. Some of the plotted curves correspond to test frequencies that extend outside the specified RF band, 72-116 GHz. In particular, for an LO setting at 80 GHz, the LSB falls across  $\sim 68.3$ -76.2 GHz, while for LO at 108 GHz the USB falls across  $\sim 111.6$ -119.7 GHz; we note that the curve with the highest measured noise in the USB channel on the upper part of the IF band includes out of RF band data. Nevertheless, the measured receiver noise is within the prescribed specification with 80% of the measured points below 50 K.

The image sideband rejection of the Band 1 2SB mixer relative to Pol. V, measured in the laboratory test cryostat using a Martin-Pupplett interferometer prior to its integration in the NOEMA Front-End, is shown in Fig. 24. The measured rejection is within specifications.

Fig. 25 and Fig. 26 give, for the NOEMA Band 1 Pol. V channel, the optimum SIS mixer bias settings versus LO

frequency and, respectively the receiver gain versus signal frequency. The receiver gain was measured by setting the variable digital attenuator of the warm IF module to 0 dB (no attenuation) and includes the full chain, from the cryostat vacuum window to the output of the warm IF module.

The receiver output power was measured for each LO frequency as a function of the IF in order to determine the IF bandpass gain fluctuation. The normalized output powers versus IF for several LO settings, given in Fig. 27, shows a peak-to-peak variation within 8 dB.

Fig. 28 and Fig. 29 show, for LO frequency tuned at 96 GHz, an example of the measured amplitude fluctuations of the IF output powers and, respectively of the Allan deviation versus time.

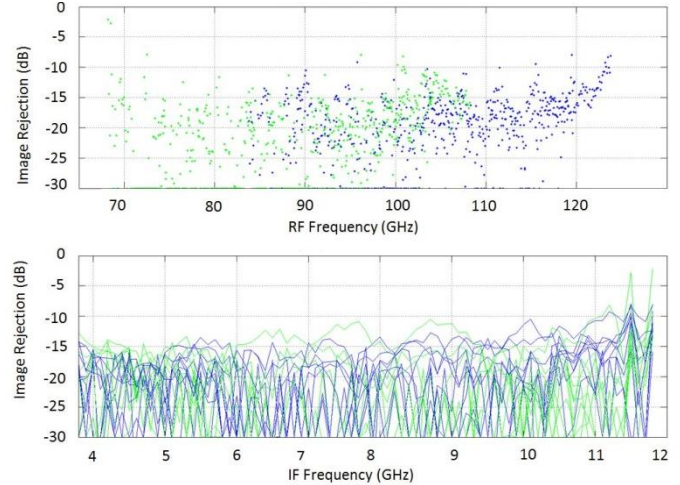


Fig. 24. Measured image band rejection of one of the Band 1 2SB mixers versus RF (top) and versus IF (bottom) for 9 different LO tunings, one every 4 GHz, from 80 GHz to 112 GHz: LSB channel (green line), USB channel (blue line).

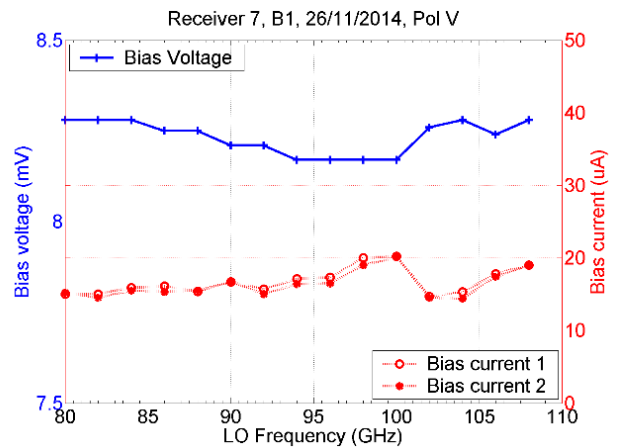


Fig. 25. Optimum bias settings for one of the NOEMA Band 1 2SB mixers (Pol. V) as a function of frequency (derived from pumped IV curves). Both DSB SIS mixers of the 2SB unit are biased at the same voltage (in the range  $\sim 8.2$ -8.3 mV for the three junction array series – blue curve, left scale) and have very similar pumped currents (in the range 15-20  $\mu$ A – red curves, right scale).

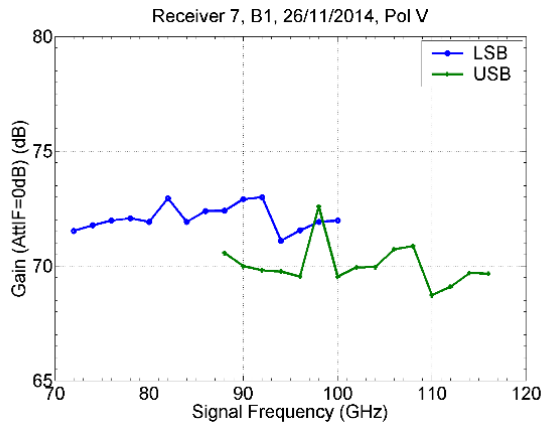


Fig. 26. LSB (blue curve) and USB (green curve) NOEMA Band 1 receiver gain versus frequency with attenuation level of the warm IF chain set to 0 dB (no attenuation).

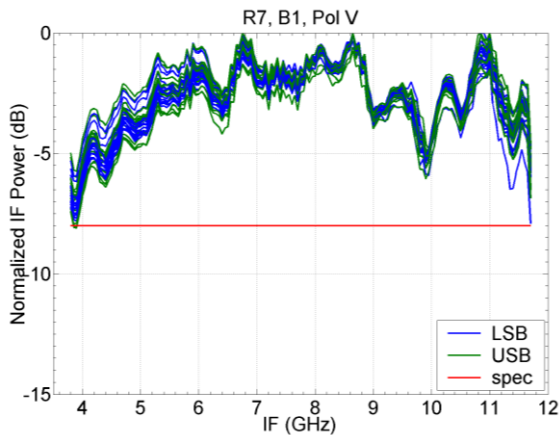


Fig. 27. Normalized IF output powers for LSB (blue curve) and USB (green curve) channels versus IF for 15 different LO settings (from 80 GHz to 108 GHz by steps of 2 GHz, 30 curves in total). The horizontal red line at -8 dB is the specification (8 dB peak-to-peak full band, see Tab. II).

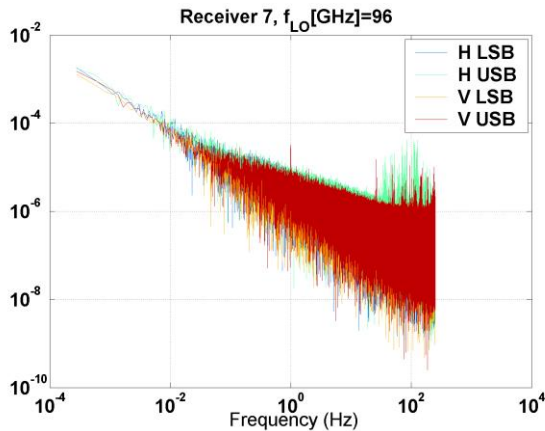


Fig. 28. Measured amplitude fluctuation of the IF output power when the NOEMA Band 1 receiver is tuned at 96 GHz LO. The four outputs (Pol. H-LSB, Pol H-USB, Pol V-LSB, Pol V-USB) are measured over the full IF bandwidth (~3.8-11.7 GHz).

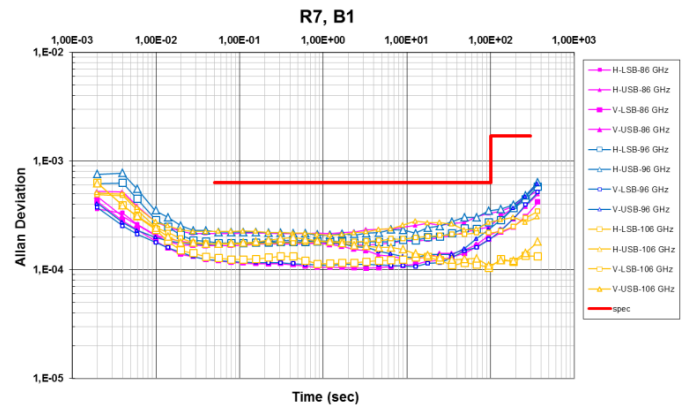


Fig. 29. Allan deviation versus time measured at three NOEMA Band 1 LO frequencies: 86 GHz (pink curves), 96 GHz (blue curves) and 106 GHz (yellow curves). For each LO setting, the four outputs (Pol. H-LSB, Pol H-USB, Pol V-LSB, Pol V-USB) are measured over the full IF bandwidth (~3.8-11.7 GHz).

### B. NOEMA Band 2 receiver characterization results

The performances of the NOEMA Band 2, Band 3 and Band 4 receivers were measured in the laboratory following the same methodology and setup adopted for NOEMA Band 1. The NOEMA Band 2 receiver noise was measured for 21 different LO frequencies across the 135-175 GHz LO range, by steps of 2 GHz. Optimum performance was obtained with bias voltages applied to the mixers in the 7.5-8.1 mV range (each DSB mixer chip utilizes a series array of three SIS junctions).

Fig. 30 shows the SSB noise temperature integrated across the IF band versus RF signal frequency of the NOEMA Band 2 (127-179 GHz) Pol. V receiver channel. The integrated SSB noise is within the 65 K specification across the full frequency band.

The image sideband rejection of the Band 2 2SB mixer relative to Pol. V, measured in the laboratory test cryostat prior to its integration in the NOEMA Front-End, is shown in Fig. 31.

The Band 2 Pol.H receiver channel has a similar performance.

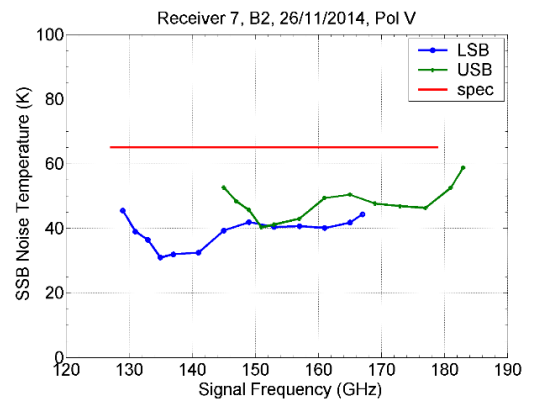


Fig. 30. SSB receiver noise temperature of the NOEMA Band 2 receiver, Pol. V, integrated across the IF band: LSB channel (blue line), USB channel (green line). The horizontal red line indicates the noise specification over 80% of the RF band.

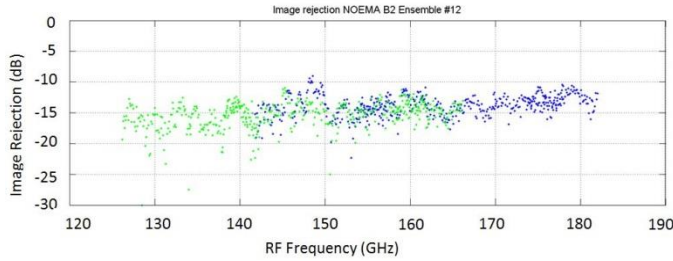


Fig. 31. Measured image band rejection of Band 2 2SB mixer versus RF for 10 different LO tunings, one every 4 GHz, from 138 GHz to 174 GHz: LSB channel (green line), USB channel (blue line).

### C. NOEMA Band 3 receiver characterization results

The NOEMA Band 3 receiver noise was measured at 16 different LO frequencies across the 207-268 GHz LO range, by steps of 4 GHz. Optimum bias conditions were found for SIS mixers biased in the 2.1-2.6 mV range and for pumping currents in the 13-30  $\mu$ A range. Fig. 32 shows the SSB noise temperature integrated across the IF band versus RF signal frequency of the NOEMA Band 3 (200-276 GHz) Pol. H receiver channel. The integrated SSB noise is within the 83 K specification across the full frequency band.

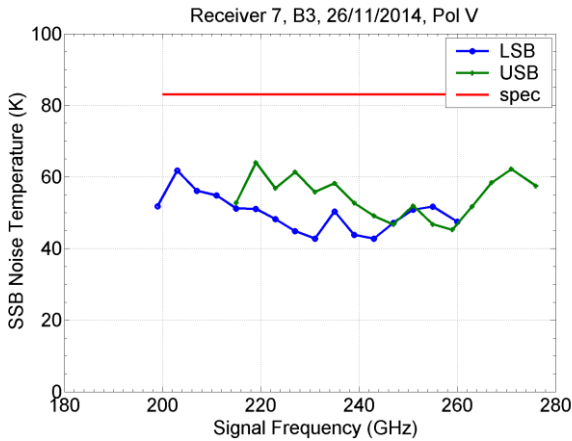


Fig. 32. SSB receiver noise temperature of the NOEMA Band 3 receiver, Pol. H, integrated across the IF band: LSB channel (blue line), USB channel (green line). The horizontal red line indicates the noise specification over 80% of the RF band.

The image sideband rejection of the Band 3 2SB mixer relative to the same polarization channel (Pol. H), measured in the laboratory test cryostat prior to its integration in the NOEMA Front-End, is shown in Fig. 33.

The Band 3 Pol. V receiver channel has a similar performance.

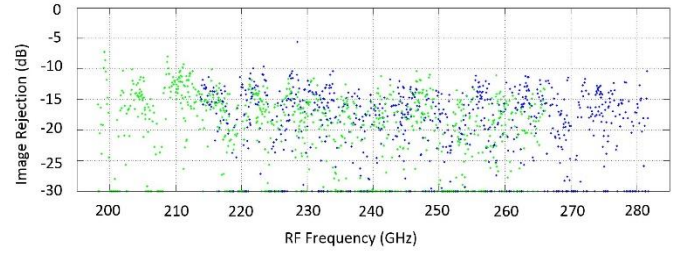


Fig. 33. Measured image band rejection of Band 3 2SB mixer versus RF for 11 different LO tunings, one every 6 GHz, from 210 GHz to 270 GHz: LSB channel (green line), USB channel (blue line).

### D. Band 4 receiver characterization results

Unlike all the other bands, neither the cryogenic module nor the 2SB mixers have been upgraded to the NOEMA requirements for Band 4. The Band 4 receiver installed in the NOEMA Ant. 7 cryostat is of the same type of those currently operating in the PdBI Front-End, i.e. based on ALMA Band 7 2SB mixers that deliver one 4 GHz wide IF band per polarization channel. Each mixer chip employs a single SIS junction.

The Band 4 receiver noise was measured at 22 different LO frequencies across the 283-365 GHz LO range, by steps of 4 GHz. Optimum performance was obtained with bias voltage on the two DSB mixers of the 2SB assembly in the range 2.1-2.5 mV and with pumped currents in the range 25-30  $\mu$ A. Fig. 34 shows the SSB noise temperature integrated across the 4-8 GHz IF band versus RF signal frequency of the Band 4 Pol. V receiver channel. The integrated SSB noise is well below the 137 K specification across the full frequency band.

The image sideband rejection of the Band 4 2SB mixer relative to the same polarization channel (Pol. H), measured in the laboratory test cryostat prior to its integration in the NOEMA Front-End, is shown in Fig. 35.

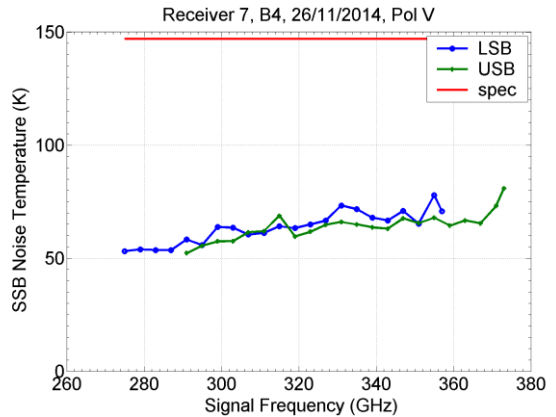


Fig. 34. SSB receiver noise temperature of the Band 4 receiver, Pol. V, integrated across the 4-8 GHz IF band: LSB channel (blue line), USB channel (green line). The horizontal red line indicates the noise specification over 80% of the RF band.

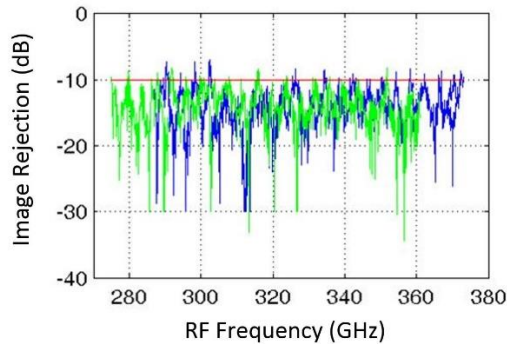


Fig. 35. Measured image band rejection of Band 4 2SB mixer versus RF for 22 different LO tunings, one every 4 GHz, from 283 GHz to 365 GHz: LSB channel (green line), USB channel (blue line).

#### NOEMA FRONT-END INSTALLATION AND ALIGNMENT

Following the successful test results obtained in the laboratory (described in previous section), the Front-End was installed and aligned in NOEMA Ant. 7 in December 2014. A photo of the Front-End and its arrangement inside the antenna receiver cabin is shown in Fig. 36.

The Front-End alignment was carried out using the same procedure successfully adopted in the past for the alignment of the EMIR and the 3 mm HEMT Front-Ends with the 30-m telescope optics: the IRAM mm-wave antenna range, based on a X-Y planar scanner with mm-wave emitter, was fixed onto the NOEMA Front-End frame in the laboratory, prior to its installation in the antenna, and the beam directions for Bands 1, 2, 3 and 4 were measured outside the cryostat vacuum windows. Then, the average orientation of the four RF beams was calculated and the beam orientation with respect to the X-Y plane of the antenna range was derived. An optical laser was fixed onto the receiver frame as to be mechanically centred on the four RF cryostat windows and its orientation was adjusted to get a laser beam parallel to the average orientation of the radio beams (by retro-reflection from an auxiliary flat mirror). Then, the laser was dismantled and packed. After installation of the NOEMA Front-End in Ant. 7, the laser was mounted back to its precise position with optical beam orientation previously derived in the laboratory. The Front-End was aligned to direct the optical laser beam, i.e. the average of the four RF beams, towards the antenna sub-reflector centre. After alignment, the laser was dismantled from the Front-End frame. The commissioning of the Ant. 7 with its Front-End, started in February 2015 and was completed in June 2015.

#### CONCLUSION

We have described the mm-wave Front-End developed at IRAM for the NOEMA project. The heterodyne Front-End has state-of-the-art performance and is based on quadri-band SIS sideband separating mixers and IF sections delivering four  $\sim 7.7$  GHz wide IF outputs. The instrument features many novelties compared to the current PdBI Front-End

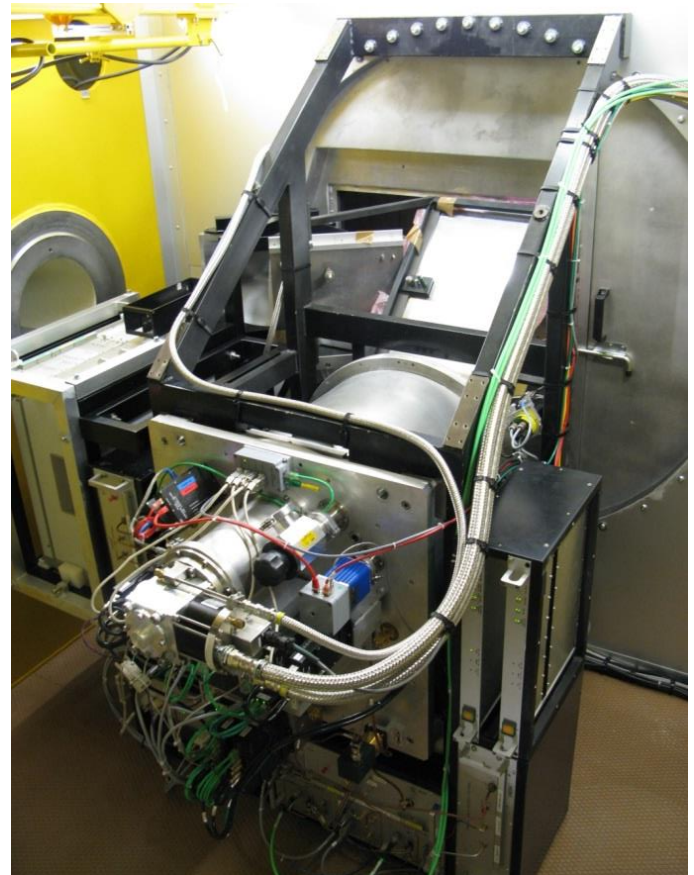


Fig. 36. View of the NOEMA Front-End installed on the Antenna 7 receiver cabin.

generation; it was successfully tested in the laboratory, then installed and aligned in Ant. 7.

#### ACKNOWLEDGMENT

We thank the IRAM Mechanical Workshop Group for their help in the mechanical design of the receiver and of its components and for the fabrication of the parts. We thank the IRAM SIS Group for the fabrication of the SIS mixer chips and of the superconducting IF hybrids.

#### REFERENCES

- [1] S. Guilloteau, J. Delannoy, D. Downes, A. Greve, M. Guelin, R. Lucas, S.J.E. Radford, J.Wink, J. Cernicharo, T. Forveille, S. Garcia-Burrillo, R. Neri, J. Blondel, A. Perrigouard, D. Plathner, M. Torres "The IRAM interferometer on Plateau de Bure," *Astronomy&Astrophysics*, Vol. 262, 624-633, 1992.
- [2] A. Wootten and A. R. Thompson, "The Atacama Large Millimeter/Submillimeter Array," *Proc. IEEE*, vol. 97, no. 8, pp. 1463-1471, Aug. 2009.
- [3] The ALMA Observatory, web page : <http://www.almaobservatory.org/>
- [4] D. Maier, S. Devoluy, M. Schicke, K. F. Schuster, "230 GHz SSB SIS mixer for Band 3 of the new generation receivers for the Plateau de Bure Interferometer," *16<sup>th</sup> Int. Symp. on Space Terahertz Tech.*, pp. 33-36, Goteborg, Sweden, May 2<sup>nd</sup>-4<sup>th</sup>, 2005.
- [5] A. Navarrini, A.L. Fontana, D. Maier, P. Serres, "Superconductor-Insulator-Superconductor Mixers for the 2 mm Band (129-174 GHz),

*Journ. of Infrared, Millimeter, and Terahertz Waves*, Vol. 35, Issue 6, pp. 536-562, July 2014.

- [6] P. Serres, A. Navarrini, Y. Bortolotti, O. Garnier, "The IF output impedance of SIS mixers," *IEEE Trans. Terahertz Sci. and Tech.*, Vol. 5, Issue 1, pp. 27-36, Jan. 2015.
- [7] D. Maier, J. Reverdy, L. Coutanson, D. Billon-Pierron, C. Boucher and A. Barbier, "Fully integrated sideband-separating Mixers for the NOEMA receivers," in *Proc. 25<sup>th</sup> Int. Symp. on Space Terahertz Tech.*, Moscow, Russia, Apr. 27-30, pp. 80-84, 2014.
- [8] S. Mahieu, D. Maier, B. Lazareff, A. Navarrini, G. Celestin, J. Chalain, D. Geoffroy, F. Laslaz, G. Perrin, "The ALMA Band-7 Cartridge," *IEEE Transactions on Terahertz Science and Technology*, Vol. E Issue 1, pp.29-39, Jan 2012.
- [9] J.Y. Chenu, D. Maier, A.-L. Fontana, G. Butin, Y. Bortolotti, F. Mattiocco, S. Mahieu, A. Navarrini, "Design of the Front-End for the NOEMA Interferometer," *24<sup>th</sup> Int. Symp. on Space Terahertz Tech., Groningen*, The Netherlands, Apr. 8<sup>th</sup>-10<sup>th</sup>, 2013.
- [10] J.Y. Chenu, A. Navarrini, Y. Bortolotti, G. Butin, A.L. Fontana, S. Mahieu, D. Maier, F. Mattiocco, P. Serres, M. Berton, O. Garnier, Q. Moutote, M. Parioleau, B. Pissard, J. Reverdy, "The NOEMA Front-End," *Proc. 26<sup>th</sup> Int. Symp. on Space Terahertz Tech.*, Cambridge, MA, USA, M3-2, Mar. 16<sup>th</sup>-18<sup>th</sup>, 2015.
- [11] M. Carter, B. Lazareff, D. Maier, J.Y. Chenu, A.-L. Fontana, Y. Bortolotti, C. Boucher, A. Navarrini, S. Blanchet, A. Greve, D. John, C. Kramer, F. Morel, S. Navarro, J. Penalver, K.F. Schuster, C. Thum, "The EMIR multi-band mm-wave receiver for the IRAM 30 m telescope," *Astronomy&Astrophysics* Vol. 538, A89, 2012.
- [12] D. Maier, J. Reverdy, D. Billon-Pierron, and A. Barbier, "Upgrade of EMIR's Band 3 and Band 4 Mixers for the IRAM 30 m Telescope," *IEEE Trans. Terahertz Science and Technology* 2, pp. 215-221, 2012.
- [13] The IRAM 30 m telescope, web pages: <http://www.iram-institute.org/EN/30-meter-telescope.php>.
- [14] F. Mattiocco, O. Garnier, D. Maier, A. Navarrini, P. Serres, "Electronically Tuned Local Oscillators for the NOEMA Interferometer," to be published in *IEEE Trans. Terahertz Science and Tech.*, 2016.
- [15] F. Mattiocco, O. Garnier, J.M. Danneel, M. Berton, D. Maier, A. Navarrini, J. Reverdy, and P. Serres, "Electronically Tuned Local Oscillators for the NOEMA Interferometer," *Proc. 26<sup>th</sup> Int. Symp. on Space Terahertz Tech.*, Cambridge, MA, USA, 16-18 March, 2015.
- [16] E. Bryerton, K. Saini, M. Morgan, M. Stogoski, T. Boyd and D. Thacker, "Development of electronically tuned local oscillators for ALMA," in *30<sup>th</sup> Int Conf on IR and MM Waves and 13<sup>th</sup> Int. Conf. on THz Elec.*, Williamsburg, USA, Sept. 19-23, 2005, vol.1, pp. 72-73.
- [17] M. Morgan, E. Bryerton, H. Karimy, D. Dugas, L. Gunter, K. Duh, X. Yang, P. Smith and P.C. Chao, "Wideband medium power amplifiers using a short gate-length GaAs MMIC process," in *IEEE MTT-S Int. Microwave Symp. Dig.*, Boston, MA, Jun. 2009, pp. 541-544.



on site of the Front-End equipments.

**Jean Yves Chenu** received a two years university degree in electronics from Institut Universitaire de Technologie, Rennes, France. From 1978 to 1985 he was with the LMT (Le Matériel Téléphonique) Radio Professionnelle involved in the assembly and testing of power transmitters for military projects. Since 1985 he has been with the Front-End Group of the Institut de RadioAstronomie Millimétrique (IRAM), Saint Martin d'Hères, France, where he is in charge of the construction, test and installation



**Alessandro Navarrini** received the S.M. degree in physics from the University of Florence, Florence, Italy, in 1996 and the Ph.D. degree in electronics and microelectronics from the Université Joseph Fourier, Saint Martin d'Hères, France, in 2002. From 1998 to 2003, he was with the Institut de Radioastronomie Millimétrique (IRAM), Saint Martin d'Hères, France, where he worked on the development of low-noise superconducting SIS receivers. From 2003 to 2006, he was Post-Doctoral Fellow with the Radio Astronomy Laboratory at the University of California, Berkeley, USA. In 2006 he joined the National Institute for Astrophysics (INAF), Cagliari Astronomy Observatory, Capoterra, Italy. From 2010 to 2015 he was with IRAM, France, where he was in charge of the Front-End Group. Since 2015 he has been with the National Institute for Astrophysics (INAF), Radio Astronomy Observatory, Cagliari, Italy. His research interests include radio astronomy instrumentation and in particular low-noise microwave and millimeter-wave receivers.



**Yves Bortolotti** received the diploma (DUT) in electronics and industrial informatics, specialized in microwave, from GE2, Université Joseph Fourier, Grenoble, France. He joined the Institut de Radioastronomie Millimétrique (IRAM), Saint Martin d'Hères, France, in 1991, and is currently working on electronics control modules design for the Front-Ends.

**Gilles Butin** received a degree in physics at the University of Paris VII in 1972, and an engineering degree in electronics at the École Supérieure d'Électricité in 1976. He worked for four years at Thomson-CSF on radiocommunication devices and for four years at Schlumberger on measurement electronics for the gas industry. He joined the Institut de RadioAstronomie Millimétrique (IRAM) in 1984. There, he was in charge of the spectrometry group at the Pico Veleta Observatory, close to Granada, Spain, and ultimately of the low-noise warm electronics for the NOEMA project at Saint Martin d'Hères, France. He retired in 2014.

**Anne Laure Fontana** received the S.M. degree in microelectronics and microwaves from the Sciences and Technologies University of Lille, Lille, France, in 2002. Since 2002, she has been with the Institut de Radioastronomie Millimétrique (IRAM), Saint Martin d'Hères, France, where she works on the design and characterization of optics system and on development of cryogenic millimeter wave receivers.

**Sylvain Mahieu** received a degree in physics from the Université Paris VII in 1995 and the MSc in microwave and solid state physics from the University of Portsmouth, England, in 1996. He spent 2½ years post-graduate experience at Rutherford Appleton Laboratory (Chilton, England). He then worked for 5 years with Motorola as RF design engineer (Basingstoke, England). He joined the Institut de Radio Astronomie Millimétrique (Grenoble) in 2003 where he was in charge of Band-7 cartridge design and fabrication. He was the ALMA Band-7 cartridge work package manager from 2009 until 2012. Since 2012, he has been playing the role of system engineer on the NOEMA project.

**Doris Maier** received the S.M. and Ph.D. degrees in physics from the University of Cologne, Cologne, Germany, in 1993 and 1996, respectively. She is currently with the Institut de Radioastronomie Millimétrique (IRAM), Saint Martin d'Hères, France, where she is working on the development of sub-millimeter wave instrumentation for radio astronomy.



**Francois Mattiocco** received the M.S. and Ph.D. degrees in electronic, instrumentation and metrology from the University of Pierre & Marie Curie, Paris, France, in 1976 and 1979 respectively. From 1980 to 1984 he was with the Thomson CSF involved in the development of parametric amplifiers for satellite communications. Since 1984, he has been in the receiver group of the Institut de RadioAstronomie Millimétrique (IRAM), Saint Martin d'Hères, France, where he

was involved in the development of millimeter devices and systems (e.g., Gunn oscillators, multipliers, harmonic mixers, centimeter radiometers for antenna holography and interferometric atmospheric phase correction). His research interest has included the development of a novel sub-millimeter Vector Network Analyzer. Now his works focuses on wide band electronically tuned millimeter local oscillators for SIS receivers used in radio astronomy.



**Bruno Pissard** received a BTS (Brevet de Technicien Supérieur) in electronics in 1988. He spent 15 years in an industrial firm working for Jay Electronique, an electronics company specialized in development and production of safety infrared sensor detection, and safety wireless remote control, where he worked as a technician in the departments of: Quality control, Quality assurance, R&D, Production, and Test laboratory. Since 2006 he has been with the Institut de Radio Astronomy Millimétrique (IRAM), Saint Martin d'Hères,

France, where he works on assembly of millimeter-wave receivers, and take part to the development of different electronics microwave systems.



**Patrice Serres** received the S.M. degree in microelectronics and microwaves from the Sciences and Technologies University of Lille, Lille, France, in 2002. Since 2002, he has been with the Institut de Radioastronomie Millimétrique (IRAM), Saint Martin d'Hères, France, where he is involved in the development of cryogenic low noise millimeter wave receivers. His work focuses particularly on SIS mixer development and on cryogenic low noise HEMT amplifier integration and tests.



**Julien Reverdy** received a diploma (DUT ) in electrical engineering and industrial computer technology from University Joseph Fourier, Saint Martin d'Heres, France, in 2001. Since 2001 he has been with IRAM, where he works on SIS mixer assembly, development of test setups, and receiver tests.

**Marylene Berton** received a BTS diploma in Electronics in 1981, Choisy le Roi, France. Since 1981 she has been with the Institut de RadioAstronomie Millimétrique (IRAM), Saint Martin d'Hères, France, where she works on construction and test of local oscillator modules, receiver characterization and maintenance.



**Olivier Garnier** received a three years university degree in electronics from Institut Universitaire de Technologie, Salon-de-Provence, France. He joined the Institut de Radioastronomie Millimétrique (IRAM), Saint Martin d'Hères, France, in 2006, and is currently working on assembly and characterization of millimeter-wave components and Front-Ends.

**Quentin Moutote** received a diploma (DUT ) in electrical engineering and industrial computer technology from University Josph Fourier, Saint Martin d'Heres, France, in 2007. Since 2007 he has been with the IRAM, where he works on SIS mixer assembly, and receiver tests.

**Magali Parioleau** received a DUT (Diplôme Universitaire de Technologie) Physical Mesures physiques (2ans ) and a DEUST (Diplôme d'Études Universitaires Scientifiques et Techniques) Techniques on Vacuum and Cryogenics at Université Paul Sabatier, Toulouse, France, respectively in 1997 and 1998. Since 2004 she is been working at IRAM on the characterization of SIS mixers and of optical modules for the IRAM Front-Ends.